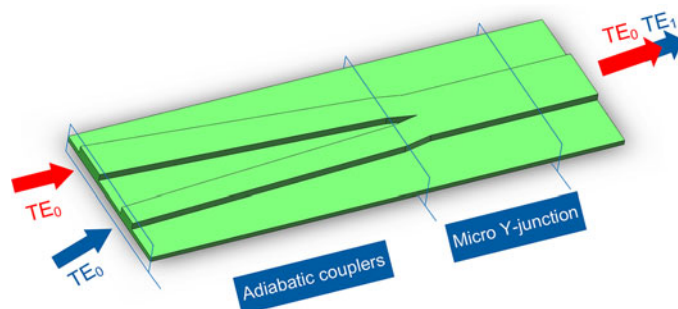


Broadband On-Chip Mode-Division Multiplexer Based on Adiabatic Couplers and Symmetric Y-Junction

Volume 9, Number 2, April 2017

Zhenrong Zhang
Yu Yu
Songnian Fu



Simple and broadband mode multiplexer

DOI: 10.1109/JPHOT.2017.2669527
1943-0655 © 2017 IEEE

Broadband On-Chip Mode-Division Multiplexer Based on Adiabatic Couplers and Symmetric Y-Junction

Zhenrong Zhang,¹ Yu Yu,² and Songnian Fu²

¹School of Computer, Electronic and Information, Guangxi University,
Nanning 530004, China

²Wuhan National Laboratory for Optoelectronics and School of Optical and Electronic Information, Huazhong University of Science and Technology, Wuhan 430074, China

DOI:10.1109/JPHOT.2017.2669527

1943-0655 © 2017 IEEE. Translations and content mining are permitted for academic research only.

Personal use is also permitted, but republication/redistribution requires IEEE permission.

See http://www.ieee.org/publications_standards/publications/rights/index.html for more information.

Manuscript received January 11, 2017; revised February 8, 2017; accepted February 12, 2017. Date of publication February 15, 2017; date of current version March 1, 2017. This work was supported by 863 High Technology Plan under Grant 2015AA015502; the National Natural Science Foundation of China under Grant 6161101303 and Grant 61661004; and the Open fund of the State Key Laboratory of Advanced Optical Communication Systems and Networks (Peking University), China. Corresponding author: Y. Yu (e-mail: yuyu@mail.hust.edu.cn).

Abstract: The mode-division multiplexer/demultiplexer (MMUX/DeMMUX) is the crucial component for the implementation of mode-division multiplexing (MDM) transmission. We propose an on-chip two-mode MMUX/DeMMUX based on adiabatic couplers. Thanks to the principle of mode evolution, the proposed MMUX possesses advantages of broadband operation and high tolerance of fabrication error. The performance is experimentally evaluated by integrating the proposed MMUX and DeMMUX into an on-chip MDM link, with a low crosstalk of <-19 dB and insertion loss of <1.5 dB over a wavelength range of 90 nm. Furthermore, reasonable performance degradation can be observed for deviations of gap and etch depth from -50 to 50 nm.

Index Terms: Waveguide devices, silicon nanophotonics.

1. Introduction

To satisfy the exponentially increasing bandwidth demand for data-intensive applications such as Exascale performance computers and datacenters, various advanced multiplexing technologies have been investigated to increase the interconnection capacity by utilizing parallel channels [1]–[5]. The wavelength-division multiplexing (WDM) is one of the most successful multiplexing technologies, and it has been extensively employed in commercial applications. However, for WDM systems, multiple laser sources are required, resulting in high cost and energy consumption. Recently, mode division multiplexing (MDM) has attracted lots of attentions, because multiple spatial modes can be simultaneously applied to further increase the spectral efficiency and capacity. The mode division multiplexer/demultiplexer (MMUX/De-MMUX) which can combine/separate the complete set of guided modes of a multimode bus waveguide/fiber is the key device for MDM implementation [6]–[14]. Many previous schemes have been reported utilizing silicon-on-insulator (SOI) platforms, for instance, asymmetric directional couplers (ADCs) [6]–[8], the multimode interference (MMI) coupler [9], [10], and the asymmetric Y-junction [11]–[14]. The ADC-based MMUX usually takes advantage of compact footprint, and it can be easily scaled up to process more modes. However, the precise

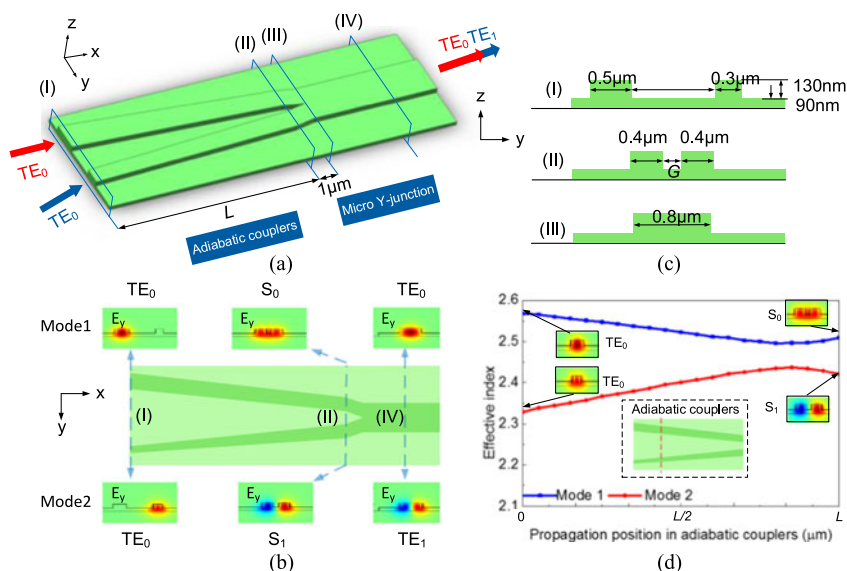


Fig. 1. (a) Three-dimensional view of the proposed MMUX, including ACs and a micro Y-junction. (b) Mode profiles at different positions along the MMUX. Two green colors refer to different layers. The dark green refers to the ridge layer, while the light one refers to the slab layer. (c) Cross-sectional view. (d) Effective indices of the two guided modes versus the propagation position at 1550 nm. (Inset) Mode profiles at both ends of the ACs.

phase matching is compulsory, and the performance is sensitive to device size variations. On the other hand, the bandwidth is typically limited to a few tens of nanometers. The MMI-based device is relatively complicated, and several MMI couplers and phase shifters are normally needed. A precise fabrication is usually required to obtain the desired ultra-small corner in asymmetric Y-junction based scheme, and it is challenging to achieve a low-loss Y-junction. On-chip MMUX scheme based on adiabatic couplers (ACs) have been proposed recently, and it exhibits wide bandwidth due to the mode evolution principle [15]. However, the multiplexed signals are transmitted in the supermode waveguide rather than a normal bus waveguide, resulting in the incompatibility with other multimode devices for MDM system.

We propose and fabricate a simple on-chip MMUX/De-MMUX consisting of ACs and a micro Y-junction. The proposed scheme is different from the previously reported one [15], a micro Y-junction is utilized to connect the ACs and normal bus waveguide, which can be used to accommodate other multimode devices such as higher order-mode pass filter [16]. In the proposed device, the angle between the branches of the micro Y-junction is much larger than that of asymmetric Y-junction, leading to a relaxation of the fabrication difficulty. Detailed theoretical investigation of the proposed MMUX is presented in order to obtain the optimal parameters. The integrated MDM link including the proposed MMUX and De-MMUX is demonstrated with crosstalk lower than -19 dB and insertion loss less than 1.5 dB over 90 nm wavelength range. Furthermore, the fabrication tolerance is investigated, indicating a good tolerance on gap and etch depth.

2. Operation Principle and Simulation

The proposed mode MMUX is presented in Fig. 1. It consists of ACs and a micro Y-junction. Actually, ACs are commonly applied in the photonics lantern and one of the advantages is wavelength insensitivity [17]–[19]. For the ACs, two single-mode waveguides with different widths and a large gap are adopted, to avoid undesired interference. Then, the different widths are tapered slowly to a same value, and the gap is decreased gradually. Thus, part of the field in one waveguide is coupled into the other. The two waveguides are closely spaced to form a coupling configuration by supporting two supermodes denoted as S_0 and S_1 [20]. Based on the operation principle of mode

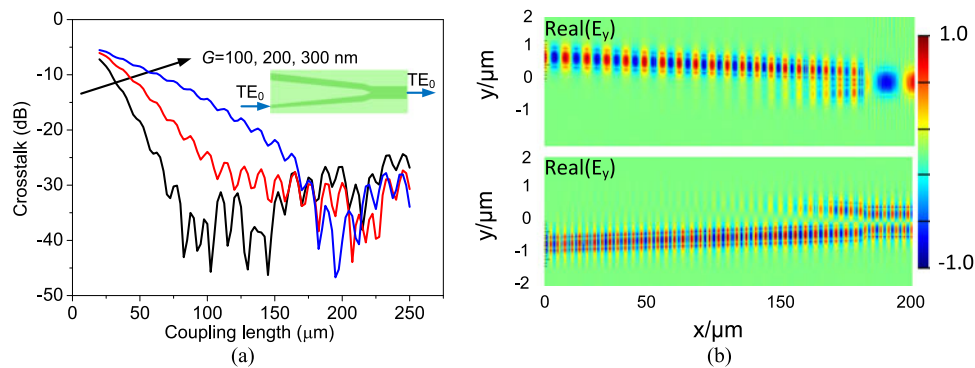


Fig. 2. (a) Calculated crosstalk at 1550 nm when the TE_0 mode is injected into the narrow waveguide. (b) Calculated field distributions at 1550 nm under conditions of the gap $G = 200$ nm and the ACs length $L = 180$ μm .

evolution in the two waveguides forming the ACs [21]–[23], one supermode can be selectively excited by launching only one normal mode from each waveguide. The mode profiles at different positions along the MMUX are shown in Fig. 1(b). After the ACs, the supermodes propagate into the micro Y-junction and then are combined into the bus waveguide. The micro Y-junction is a symmetrical structure, and the branches consist of two very short single-mode waveguides with same width. According to the symmetry principle, when the symmetric mode S_0 is injected into the micro Y-junction, only TE_0 mode can be excited. Similarly, the anti-symmetric mode S_1 only excites the TE_1 mode. The working mechanism of symmetric Y-junctions can be also described as the even and odd supermode evolution from the stem of the micro Y-junction to the output [21], [22].

The MMUX is designed on SOI wafer with 220 nm top silicon, and the SiO_2 cladding is adopted to the entire device. To reduce the reflection at the corner between the two waveguides with 130 nm ridge height are utilized to constitute the device. Compared with strip waveguide, the ridge waveguide has lower propagation loss since it is less sensitive to sidewall roughness. In addition, more compact design and tolerant fabrication can be realized for the ridge-waveguide-based device. The waveguide cross sections at the main sections are exhibited in Fig. 1(c). The two waveguides of the ACs are tapered from 0.5 and 0.3 to 0.4 μm linearly. On the other hand, the gap between them is decreased from 1 μm to various values (G) along the coupling length L . The width and length of the branch part of the micro Y-junction are 0.4 and 1 μm , respectively. The width of the bus waveguide is set as 0.8 μm . To further explore the mode evolution, the effective indices of the two guided modes in different positions along the propagation direction by the finite difference algorithm are calculated, as shown in Fig. 1(d). The mode profiles at both ends of the ACs are also presented as the insets of Fig. 1(d). One can see that the TE_0 mode injected into the wide waveguide evolves into S_0 mode, due to the closely matched effective index. In contrast, the TE_0 mode launching from the narrow branch converts into the S_1 mode.

The crosstalk with respect to the coupling length L of the ACs is calculated in Fig. 2(a), for three different gaps ($G = 100, 200, 300$ nm) at 1550 nm. Here, the crosstalk is defined as the power ratio of the output TE_0 mode to the TE_1 in the bus waveguide, when light is injected from the narrow waveguide. For a fixed length, it can be seen that the crosstalk decreases with the reduction of gap G . On the other hand, the crosstalk can be very low when L is larger than 150 μm . The same results can also be obtained, when light is launching from the wide waveguide. In our design, $G = 200$ nm and $L = 180$ μm are utilized, by taking into account both crosstalk and device footprint. Although a more compact design is possible under the condition of a smaller G , the fabrication difficulty is increased greatly. To be noted, the angle between the branches of the Y-junction is 11.4 degrees, which is much larger than that of traditional asymmetric Y-junction (~ 1 degree) [11], leading to a relaxation of the fabrication difficulty. The calculated electric field distributions are shown in Fig. 2(b). When TE_0 mode is launched from the wide input, a TE_0 mode is observed. Alternatively, a TE_1

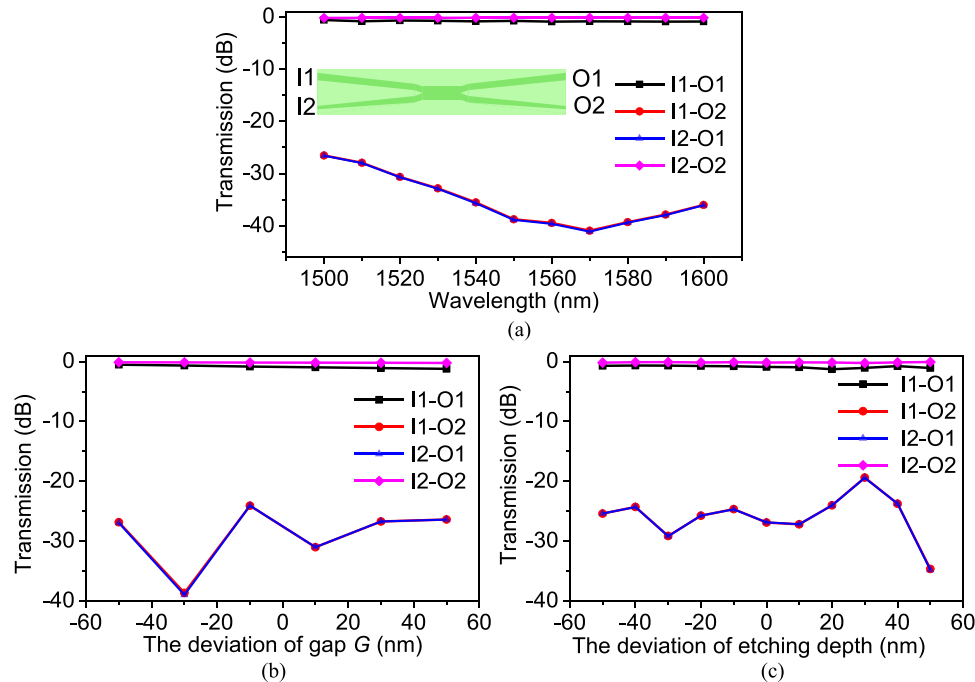


Fig. 3. (a) Calculated transmission spectra of the MDM link. (Inset) MDM link covering the mode MUX and DeMMUX. The length of the bus waveguide is $20 \mu\text{m}$. Calculated transmission of the MDM link versus (b) the gap G and (c) the etch depth deviations at 1550 nm .

mode can be obtained in case the TE_0 is injected from the narrow input. Thus, the mode multiplexed signals are achieved in the bus waveguide. The bidirectional eigenmode expansion (EME) method is utilized to obtain the electric field distributions.

Next, the bandwidth performance of the proposed MDM link is also calculated by the EME method, as shown in Fig. 3(a). The EME algorithm has been extensively verified as a precise and effective method for simulating light propagation over long distances [24], [25]. The schematic of a full MDM link containing two of the proposed designs acting as MMUX and De-MMUX is also shown, with two input ports (I1 & I2) and two output ports (O1 & O2), respectively. The MMUX has the same parameters with the De-MMUX, and a straight bus waveguide with $20 \mu\text{m}$ length is used to connect them. The legend “I2-O1” in Fig. 3(a) refers to the transmission from input port I2 to output port O1. The insertion loss at output port O1 is $\sim 0.9 \text{ dB}$ from 1500 to 1600 nm , and the crosstalk (transmission path for I2-O1) is $< -26 \text{ dB}$. The insertion loss at output port O2 is $\sim 0.2 \text{ dB}$, and the crosstalk (transmission path for I1-O2) is $< -26 \text{ dB}$. Thus, a high extinction ratio of more than 25 dB over a range of 100 nm can be obtained, ensuring good performance for MDM operation. The insertion loss difference between two output ports may be due to larger reflection at the corner of the micro Y-junction, because TE_0 mode has stronger electric field intensity in the center of the waveguide than that of TE_1 mode. The transmission curves as functions of gap G and the etch depth are calculated at 1550 nm , respectively. A crosstalk $\sim -26 \text{ dB}$ can be ensured when the gap G deviation is from -50 to 50 nm , as shown in Fig. 3(b). The crosstalk also keeps $\sim -25 \text{ dB}$ when the etch depth deviation is from -50 to 50 nm , as shown in Fig. 3(c). Consequently, large fabrication tolerance is possible, and thus, a good reliability of the proposed MMUX can be guaranteed.

3. Device Fabrication and Experimental Results

The proposed device was fabricated by the 248 nm deep ultraviolet lithography. Two etch masks are chosen to pattern the wafer: one etch depth of 70 nm for the grating couplers (GCs) and the other etch depth of 130 nm for the waveguides. The inductively coupled plasma (ICP) etch is

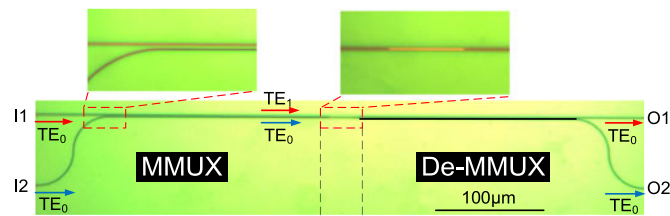


Fig. 4. Microscope views of the fabricated MDM link including MMUX and DeMMUX.

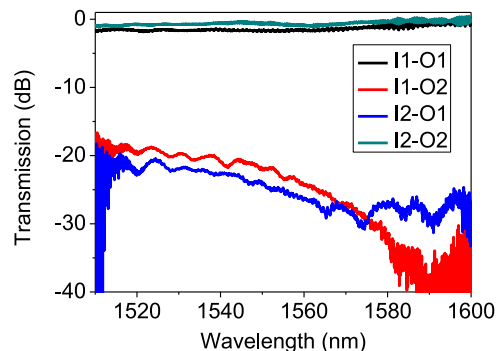


Fig. 5. Measured transmission spectra of the MDM link.

applied to form the structure. Fig. 4 shows the microscope views of the fabricated MDM link. The zoom-in pictures of the ACs, micro Y-junction are also exhibited as insets. In order to evaluate the performance of the fabricated MDM link, the transmission spectra are measured by coupling the light from a broadband source into the device by a TE grating coupler (GC), as shown in Fig. 5. A set of reference circuits with only GCs connected with a straight waveguide have been fabricated on the same chip. The spectra are normalized by subtracting the loss induced by the GCs, showing that the modal crosstalk (transmission paths for I1-O2 and I2-O1) is lower than -19 dB and insertion loss (transmission paths for I1-O1 and I2-O2) is less than 1.5 dB from 1510 to 1600 nm. It is worth mentioning that the drastic oscillations around 1510 and 1600 nm result from the severe reduction of the light intensity from the broadband source, as well as the low coupling efficiency of the GCs. The real bandwidth performance can be obtained if a wider light source and a better coupling design such as edge coupling are applied. Although the proposed scheme is not easy to scale up for more modes, it is still meaningful due to large bandwidth and fabrication tolerance.

4. Conclusion

We have proposed and demonstrated a simple two-mode multiplexing scheme based on adiabatic couplers. To relax fabrication difficulty, a micro Y-junction is adopted to connect the adiabatic couplers and normal bus waveguide, enabling the compatibility with other multimode devices. The MDM link including the proposed MMUX and DeMMUX is characterized with crosstalk lower than -19 dB and insertion loss of less than 1.5 dB over 90 nm wavelength. The fabrication tolerance is also investigated, indicating a good reliability of the proposed mode MUX on the gap and etching depth deviations.

References

- [1] P. De Heyn *et al.*, "Polarization-insensitive 5×20 Gb/s WDM Ge receiver using compact Si ring filters with collective thermal tuning," in *Proc. Opt. Fiber Commun. Conf.*, 2014, Art. no. Th4C.5.

- [2] P. Verheyen *et al.*, "Highly uniform 25 Gb/s Si photonics platform for high-density, low-power WDM optical interconnects," in *Proc. Integr. Photon. Res. Conf.*, 2014, Art. no. IW3A.4.
- [3] K. Chen *et al.*, "Wavelength-multiplexed duplex transceiver based on III-V/Si hybrid integration for off-chip and on-chip optical interconnects," *IEEE Photon. J.*, vol. 8, no. 1, Feb. 2016, Art. no. 7900910.
- [4] C. R. Doerr and T. F. Taunay, "Silicon photonics core-, wavelength-, and polarization-diversity receiver," *IEEE Photon. Technol. Lett.*, vol. 23, no. 9, pp. 597–599, May 2011.
- [5] D. Dai, J. Wang, S. Chen, S. Wang, and S. He, "Monolithically integrated 64-channel silicon hybrid demultiplexer enabling simultaneous wavelength and mode-division-multiplexing," *Laser Photon. Rev.*, vol. 9, no. 3, pp. 339–344, 2015.
- [6] L.-W. Luo *et al.*, "WDM-compatible mode-division multiplexing on a silicon chip," *Nature Commun.*, vol. 5, 2014, Art. no. 3069.
- [7] C. Sun, Y. Yu, G. Chen, and X. Zhang, "Silicon mode multiplexer processing dual-path mode-division multiplexing signals," *Opt. Lett.*, vol. 41, no. 23, pp. 5511–5514, 2016.
- [8] Y. Yu, M. Ye, and S. Fu, "On-chip polarization controlled mode converter with capability of WDM operation," *IEEE Photon. Technol. Lett.*, vol. 27, no. 18, pp. 1957–1960, Sep. 15, 2015.
- [9] Y. Li, C. Li, C. Li, B. Cheng, and C. Xue, "Compact two-mode (de)multiplexer based on symmetric Y-junction and multimode interference waveguides," *Opt. Exp.*, vol. 22, no. 5, pp. 5781–5786, 2014.
- [10] T. Uematsu, Y. Ishizaka, Y. Kawaguchi, K. Saitoh, and M. Koshiba, "Design of a compact two-mode multi/demultiplexer consisting of multimode interference waveguides and a wavelength-insensitive phase shifter for mode-division multiplexing transmission," *J. Lightw. Technol.*, vol. 30, no. 15, pp. 2421–2426, Aug. 2012.
- [11] J. B. Driscoll, R. R. Grote, B. Souhan, J. I. Dadap, M. Lu, and R. M. Osgood, "Asymmetric Y junctions in silicon waveguides for on-chip mode-division multiplexing," *Opt. Lett.*, vol. 38, no. 11, pp. 1854–1856, 2013.
- [12] W. W. Chen, P. J. Wang, and J. Y. Yang, "Mode multi/demultiplexer based on cascaded asymmetric Y-junctions," *Opt. Exp.*, vol. 21, no. 21, pp. 25113–25119, 2013.
- [13] W. Chen, P. Wang, and J. Yang, "Optical mode interleaver based on the asymmetric multimode Y junction," *IEEE Photon. Technol. Lett.*, vol. 26, no. 20, pp. 2043–2046, Oct. 15, 2014.
- [14] W. Chen *et al.*, "Silicon three-mode (de) multiplexer based on cascaded asymmetric Y junctions," *Opt. Lett.*, vol. 41, no. 12, pp. 2851–2854, 2016.
- [15] J. Xing, Z. Li, X. Xiao, J. Yu, and Y. Yu, "Two-mode multiplexer and demultiplexer based on adiabatic couplers," *Opt. Lett.*, vol. 38, no. 17, pp. 3468–3470, 2013.
- [16] X. Guan, Y. Ding, and L. Frandsen, "Ultra-compact broadband higher order-mode pass filter fabricated in a silicon waveguide for multimode photonics," *Opt. Lett.*, vol. 40, no. 16, pp. 3893–3896, 2015.
- [17] D. Noordegraaf, P. M. W. Skovgaard, M. D. Nielsen, and J. Bland-Hawthorn, "Efficient multi-mode to single-mode coupling in a photonic lantern," *Opt. Exp.*, vol. 17, no. 3, pp. 1988–1994, 2009.
- [18] D. Noordegraaf *et al.*, "Multi-mode to single-mode conversion in a 61 port photonic lantern," *Opt. Exp.*, vol. 18, no. 5, pp. 4673–4678, 2010.
- [19] R. Ryf, N. K. Fontaine, and R. J. Essiambre, "Spot-based mode couplers for mode-multiplexed transmission in few-mode fiber," in *Proc. Photon. Soc. Summer Topical Meeting Ser.*, Jul. 9–11, 2012, pp. 199–200.
- [20] J. J. Xing *et al.*, "Silicon-on-insulator-based adiabatic splitter with simultaneous tapering of velocity and coupling," *Opt. Lett.*, vol. 38, no. 13, pp. 2221–2223, 2013.
- [21] J. Love and N. Riesen, "Single-, few-, and multimode Y-junctions," *J. Lightw. Technol.*, vol. 30, no. 3, pp. 304–309, Feb. 2012.
- [22] N. Riesen and J. D. Love, "Design of mode-sorting asymmetric Y-junctions," *Appl. Opt.*, vol. 51, no. 15, pp. 2778–2783, 2012.
- [23] N. Riesen and J. D. Love, "Tapered velocity mode-selective couplers," *J. Lightw. Technol.*, vol. 31, no. 13, pp. 2163–2169, Jul. 2013.
- [24] Y. Sun, Y. Xiong, and N. Y. Winnie, "Experimental demonstration of a two-mode (de) multiplexer based on a taper-etched directional coupler," *Opt. Lett.*, vol. 41, no. 16, pp. 3743–3746, 2016.
- [25] H. Xu and Y. Shi, "Dual-mode waveguide crossing utilizing taper-assisted multimode-interference couplers," *Opt. Lett.*, vol. 41, no. 22, pp. 5381–5384, 2016.